Broadband light absorption using metallic nanowire based perfect absorbers

A Dissertation submitted towards the partial fulfilment of the requirement for the award of degree of

Master of Technology in
Microwave and Optical Communication Engineering

Submitted by
Sanjivanee
2K14/MOC/16

Under the supervision of
Dr. Yogita Kalra
Assistant Professor

Department of Applied Physics and Department of Electronics & Communication Engineering

Delhi Technological University
(Formerly Delhi College of Engineering)

DECEMBER 2016

DELHI TECHNOLOGICAL UNIVERSITY

Established by Govt. of Delhi vide Act 6 of 2009
(*Formerly Delhi College of Engineering)*
SHAHBAD DAULATPUR, BAWANA ROAD, DELHI-110042

CERTIFICATE

This is to certify that the work which is being presented in the dissertation entitled "**Broadband light absorption using metallic nanowire based perfect absorbers**" is the authentic work of **Sanjivanee** under my guidance and supervision in the partial fulfilment of requirement towards the degree of Master of Technology in Microwave and Optical Communication Engineering jointly run by Department of Applied Physics and Department of Electronics & Communication Engineering in Delhi Technological University during the 2014-16.

Prof. S. C. Sharma
(Head of Department)
Department of Applied Physics

Dr. Yogita Kalra
(Supervisor)
Department of Applied Physics

DECLARATION

I hereby declare that all the information in this document has been obtained and presented in accordance with academic rules and ethical conduct. This report is my own, unaided work. I have fully cited and referenced all material and results that are not original to this work. It is being submitted for the degree of Master of Technology in Microwave and Optical Communication Engineering at Delhi Technological University. It has not been submitted by me for any degree or examination in any other university.

Sanjivanee
M. Tech, MOCE
2K14/MOC/16

ABSTRACT

Resonant plasmonics enable us to control the fundamental optical processes like absorption, emission and refraction at nanoscale. Cutting down the Fresnel Losses in nanophotonics is a challenge. Metal – insulator – metal stack in which nanostructured top silver film is designed in which metallice nanowire based (60 nm and 120 nm) super absorber yields broadband and TM and TE polarization exited resonant light absorption over the entire visible spectrum (400 – 700 nm) with an average measured absorption of 0.95.

ACKNOWLEDGEMENT

I take this opportunity as a privilege to thank all individuals who have supported and guided me.

First I would like to express my deepest gratitude to my supervisor **Dr. Yogita Kalra**, Asst. Professor, Department of Applied Physics, for her valuable support, patience, guidance, motivation and encouragement throughout the period this work was carried out. I would also like to thank Nishant Shankhwar, Research Scholar, for valuable time and interest in this project. I am grateful to both for closely monitoring my progress and providing me with timely and important advice, their valued suggestions and inputs during the course of the project work.

I am deeply grateful to the **Prof. S. C. Sharma** (Head of the Applied Physics Department), **Dr. S. Indu** (Head of the Electronics and Communication Engineering Department), **Prof. R. K. Sinha**, **Prof. Rajiv Kapoor** and **Dr. Ajeet Kumar** for their support for providing best educational facilities.

I also wish to express my heartfelt thanks to the classmates as well as staff at Department of Applied Physics and Department of Electronics & Communication of Delhi Technological University for their goodwill and support that helped me a lot in successful completion of this project.

Finally, I want to thank my parents, brother and friends for always believing in my abilities and for always showering their invaluable love and support.

Sanjivanee
M. Tech. MOC
2K14/MOC/16

LIST OF CONTENTS

LIST OF FIGURES

Fig **Caption** **Page no**

Chapter 1

Introduction

1.1. Thesis Approach:

This thesis consists of the design of perfect ultrathin absorbers capable of absorbing the radiation entire visible spectrum and to study characteristics of the absorbers based on plasmonics. The simulations and calculations of the absorber nanostructure have been realized using commercial software 'COMSOL Multiphysics' which is based on finite element method. The finite element method is used to calculate the reflection and transmission in the structure which further used to calculate the absorption. Plasmonic absorber has been studied.

1.2. Thesis Objectives:

The main objectives of the thesis are given as follows:

Study of the basics of absorption and plasmonics, different possible absorbers and its applications in the optical field.

Study and analyse the nanostructures and use of plasmonics in guiding the light through them.

Design and analysis of Broadband light absorption using metallic nanowire based perfect absorbers.

Study of dependence of the width of the absorber on absorbed power in various frequencies and design a structure that is capable to absorb at all frequencies i.e entire visible spectrum (400 nm – 700 nm).

1.3. Thesis Organization:

The outcome of the work carried out in this project is organized in six chapters. Chapter 1 consists of the overview and objective of the thesis. Chapter 2 includes the understanding of the plasmonics and nanostructures and basics of plasmonics, absorption and how light interacts

with matter resulting in absorption. Chapter 3 includes study of absorbers present and operational principle for the process. Chapter 4 deals with method that can be used for the simulation of the design proposed. Chapter 5 deals with Broadband light absorption using metallic nanowire based perfect absorbers. The project work is concluded in Chapter 6 explaining the future scope of the work that can be done on this project.

Chapter 2

Nanostructures and Photonics

2.1 Introduction

Conversion of energy has been the force driving many areas of research, one such being material science. In order to optimize the use of energy in the form of electromagnetic radiation by converting the same to other forms of energy, material scientists have slowly evolved over the search of naturally occurring substances and materials to actually synthesizing and proposing synthetic composite materials with structures such that they exhibit properties not usually found in natural materials. Structural Engineering in the form of photonic crystals, nanostructured and micro structured materials allow us to engineer the flow of energy in many desired ways, which otherwise have not been spotted as natural occurrences.

For example, photonic crystal structures have been found to have interesting applications in cloaking, slow-light, resonant cavities, lasing, reflectors and novel wave guiding. Similarly, Nano-structured arrays have also found very interesting mechanical, electrical and optical properties which were absent in the more natural bulk form of the same. The boom of the Silicon nanowire research is also a testimony to the same. In the recent times, it has been reported that resonant photonic, plasmonic and metamaterial structures allow for control of fundamental optical processes such as absorption, emission and refraction at the nanoscale. Recently a study by the Joannopolus et al. showed a control over the directionality of light by a periodic variation of electric permittivity and magnetic permeability. The Harry Atwaters .et al. opened the gates to a promising field by demonstrating that nanowired arrayed p-n junctions stand as good candidates for photovoltaic applications, but cutting down the ‘Fresnel Losses’ as well as improving the matter-radiation interaction area. T. F. Krauss et al have shown that such nano-structured semiconductors can increase the light matter interacting manifold and can have very interesting applications in slowlight, lasing and near field scanning optical microscopy, many of which were always considered to be purely in the non-linear optical regime.

In the goal to maximize the conversion of radiation energy, the first step is absorption. The regular planar bulk materials have strong reflection losses, which is also polarization

dependent. To, reduce the same, people started working on texturized surfaces and a need was felt to search for mechanisms which could increase the harvest of radiation. Nano and micro-structuring, paved the path to wave guidance, which allowed for increased coupling of energy and thus effective harvesting. This has been further enhanced by the presence of Plasmon polaritons, which provide the additional momentum to aid the process of efficient resonant energy transfer.

In the present work, we have studied an ultrathin plasmonic structure, textured and engineered to work as a 'black' super absorber!

2.2. Interaction of wave with matter

Maxwell's Equations describes the propagation of electromagnetic (EM) waves in media and its interaction with matter.

Maxwell's equations are as follows –

1. $\nabla . D = \rho$ Gauss law
2. $\nabla . B = 0$ As magnetic monopole does not exist
3. $\nabla \times E = -\frac{\partial B}{\partial t}$ As per Faraday's law
4. $\nabla \times H = J + \frac{\partial D}{\partial t}$ As per Maxwell-Ampere's law

Here,

E and D is electric field and electric displacement.

H and B are magnetic field and magnetic induction

ρ and J are charge and current densities.

D, B, and J fulfill the constitutive (or material) conditions:

$$D = \varepsilon E$$

$$B = \mu H$$

$$J = \sigma E$$

Here ε is representing electric permittivity, μ is representing magnetic permeability, and σ is representing the electrical Conductivity.

If medium is anisotropic then three quantities (ε,μ,σ) can be considered as second-rank tensor But for isotropic media, respective fields also play a role for these quantities.

$$\varepsilon = \varepsilon E$$

$$\mu = \mu H$$

$$\sigma = \sigma E$$

On expansion of permittivity as a function of Electric field $\varepsilon = \varepsilon(E) = \varepsilon_0 + \varepsilon_1 E + \varepsilon_2 E_2 + \varepsilon_3 E_3 + \varepsilon_4 E_4 + \ldots$.

The higher terms signify the nonlinear effects in EM waves.

In materials usually ε_0 dominates as long as E is not too strong such that higher orders cannot be neglected.

Let a EM wave with angular frequency, ω, wave vector k, propagating through free space. For vacuum $\rho = 0$ and $J = 0$.

Also,

$D = \varepsilon_0 E$ and $B = \mu_0 H$ ($\varepsilon 0$ and $\mu 0$ are the electrical permittivity and the magnetic Permeability in free space)

Now the Maxwell's equations can be written as –

1. $\nabla . D = 0$
2. $\nabla . B = 0$
3. $\nabla \times E = -\frac{\partial B}{\partial t}$
4. $\nabla \times H = \varepsilon_0 \mu_0 \frac{\partial D}{\partial t}$

The first two conditions need $E \perp K$ and second $B \perp K$.

Taking curl both sides,

$$\nabla \times \nabla \times E = \nabla \times \left(-\frac{\partial B}{\partial t}\right) = \frac{\partial (\nabla \times B)}{\partial t} = -\varepsilon_0 \mu_0 \frac{\partial 2E}{\partial t2}$$

∵

$$\nabla \times \nabla \times E = \nabla (\nabla . E) - \nabla^2 E$$

So the wave equation can be shown as –

For Electric Field,

$$\nabla^2 E = \varepsilon_0 \mu_0 \frac{\partial^2 E}{\partial t^2}$$

For magnetic Field,

$$\nabla^2 B = \varepsilon_0 \mu_0 \frac{\partial^2 B}{\partial t^2}$$

∵ $$\varepsilon_0 \mu_0 = \frac{1}{c^2}$$

c is the speed of light in vacuum.

When light travels through matter, these equations are altered because $\rho \neq 0$ and $J \neq 0$.

$$\frac{1}{c^2}\frac{\partial 2E}{\partial t2} - \nabla^2 E = \left(-\frac{1}{\varepsilon_0}\nabla\rho + \mu_0 \frac{\partial J}{\partial t}\right)$$

Magnetic counterpart becomes

$$\frac{1}{c^2}\frac{\partial^2 B}{\partial t^2} - \nabla^2 B = \mu_0 \nabla \times J$$

scaler (ϕ) and vector (A) potentials are related as follows-

$$E = -\nabla \phi - \frac{\partial A}{\partial t}$$

$$B = \nabla \times A$$

Ampere law becomes

$$\nabla^2 A - \frac{1}{c^2}\frac{\partial^2 A}{\partial t^2} - \nabla\left(-\frac{1}{c^2}\frac{\partial \phi}{\partial t} + \nabla . A\right) = -\mu_0 J$$

Gauss law for electricity becomes

$$\nabla^2 \phi + \frac{\partial(\nabla . A)}{\partial t} = -\frac{\rho}{\varepsilon_0}$$

Using Lorentz gauge

$$\nabla^2 A - \frac{1}{c^2}\frac{\partial^2 A}{\partial t^2} = -\mu_0 J$$

Solution can be calculated as –

$$\Phi(r,t) = \frac{1}{4\pi\varepsilon_0}\int \frac{\rho(r',t')}{|r-r\prime|}\ \delta(t)\, d^3 r' dt'$$

$$A(r,t) = \frac{\mu_0}{4\pi}\int \frac{J(r',t')}{|r-r\prime|}\,\delta(t)\, d^3 r' dt'$$

$\delta(t)$ is the dirac delta function with $t = t' + \frac{|r-r'|\prime}{nc} - t$.

n is refractive index of medium. The potentials at a certain point r and a certain time t are determined by the stimuli originating from all source points r's.

Boundary Conditions we do not have infinite medium so medium should have the definite boundaries where it interact with the other media.

2.3. Plasmonics

In plasmonics, we study the interaction of electromagnetic waves with the free electrons in the metal. Electric component of EM wave excites the free electrons.

What is Plasmon?

Plasmon can be defined as the quantized collection of longitudinal excitation of a conducting electron gas in metals.

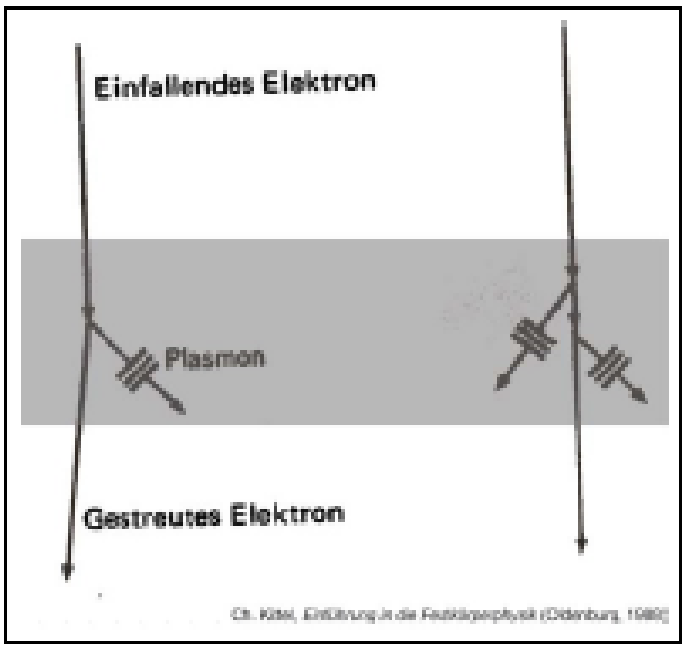

Fig 2. 1:Showing interaction of electron with metal film

Plasmon can be excited by interaction of an electron passing by a thin metal or through reflecting a photon or an electron through a metal film. Fig. 2.1 is shows interaction of electron with thin metal film which results in one or two Plasmon and one or two Plasmon.
Maxwell's equations have been used earlier to study the interaction of metals with EM fields.

In fact, the nanostructures of the size of nanostructures can also be studied using Maxwell's Equation without using quantum mechanics. As the free carriers have high density, the energy gap between the electron energy levels is very small as compared to thermal excitation energy kBT.
Optical properties are frequency dependent.

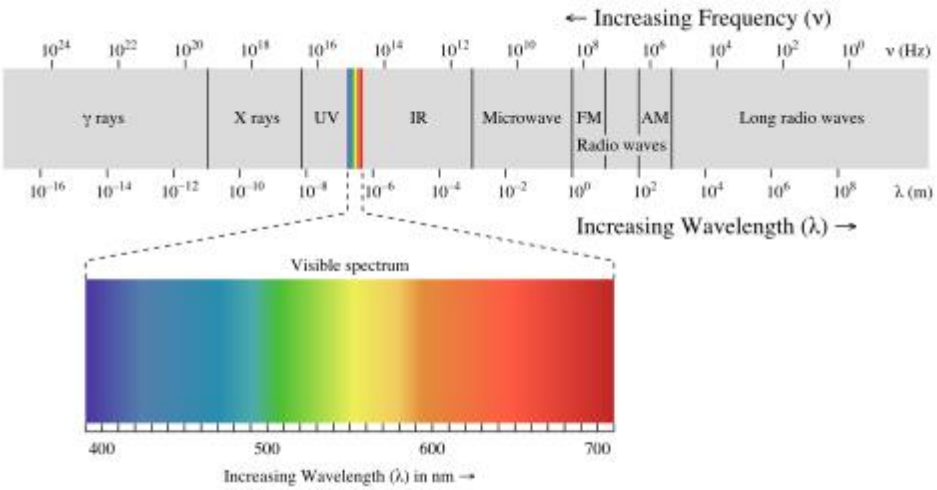

Fig 2. 2:Electromagnetic Spectrum showing visible spectrum

- For frequency up to the visible spectrum, metals are highly reflective and no EM waves can propagate through them.
- For higher frequencies like near-infrared and visible spectrum, dissipation is more as field penetration increases.
- At UV-region, metals have dielectric behavior, permitting the penetration of EM waves. Electronic band structures define amount of attenuation.

Absorption in plasmonic absorber is because of LSPR which is due to the interaction of metallic nanoparticles with the electromagnetic wave.

By surface Plasmon polaritons (SPPs), sub-wavelength confinement of light field, we are able to generate mixed wave of light and collective free electron oscillation on the metal surface which is provide advantage to plasmonics. One of the promising aspects of plasmonics is their ability to confine and channel light in sub-wavelength structures, which can be used for the miniature plasmonic circuits of order of electronic circuits.

At metal-dielectric interface collective oscillation wave of electrons called surface plasmon polariton (SPP) offers to squeeze light into nanoscale regions smaller than the wavelength of light.

SPP (Surface Plasmon Polariton)

SPP or Surface Plasmon Polariton is the waves that travel along metal- dielectric or metal- air interface. The motion of charge oscillation is involved.

The SPP are guided the same way on the interface as the light is guided in optical fiber just that SPPs are shorter in wavelength as compared to the incident light i.e. photons wavelength. So they have dense spatial confinement and higher filed intensity. They have confinement at subwavelength level perpendicular to the interface. The SPP will be guided along the interface until its energy is lost in either absorption in metal surface or in scattering in to other directions (for example free space).

Excitation of Surface Plasmon

Excitation of SPP can be done by either photons or electrons. Electrons are fired in the bulk of metal to excite the SPPs. Electrons scatter and the energy is transferred to bulk Plasma. The parallel component of scattering vector leads to the formation of surface Plasmon resonance.

To excite SPP by photon, they must have the same frequency and momenta although SPPs have high momentum due to dispersion and due to this difference in momentum the photon from air cannot directly couple to the surface. Due to the same cause the SPP on plane metal surface cannot emit energy in the form of free space photons in to the dielectric.

Dispersion relations

The electromagnetic wave can be represented as –

$E = E_0 \exp [i(k_z x + k_z z - \omega t)]$

Here k is wavenumber and ω is frequency of wave

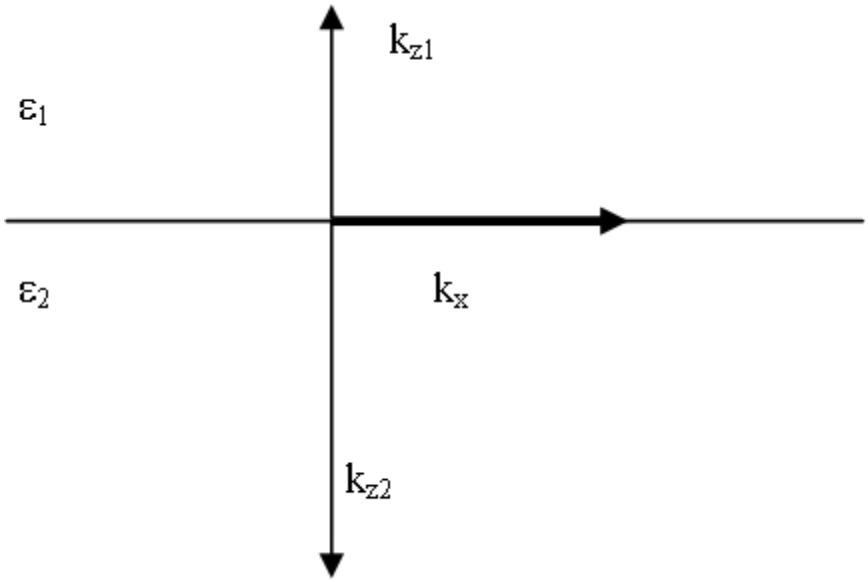

Fig 2. 3: Coordinate system to show interaction between two systems

So by solving the Maxwell equations at the interface of two materials with relative Permittivity ε_1 and ε_2 (as shown in figure 2.3), the continuity relation is as follows –

$$\frac{K_{z1}}{\varepsilon_1} + \frac{K_{z1}}{\varepsilon_2} = 0$$

And

$$K^2_x + K^2_{zi} = \varepsilon_i \left(\frac{\omega}{c}\right)^2 \quad i = 1,2\ldots$$

c is the speed of light in vaccum and k_x is similar for mediums.

Solving we get,

$$k_z = \frac{\omega}{c} \left(\frac{\varepsilon_1 \varepsilon_2}{\varepsilon_1 + \varepsilon_2}\right)^{1/2}$$

If we neglect attenuation, the permittivity in free electron model of gas is

$$\varepsilon(\omega) = 1 - \frac{\omega_2 p}{\omega_2}$$

Where, ω_p is the bulk Plasmon frequency.

And

$$\omega_p = \sqrt[2]{\frac{ne2}{\varepsilon 0 m*}}$$

n = electron density

m*= effective mass of electron.

ε_0 = permittivity of free space.

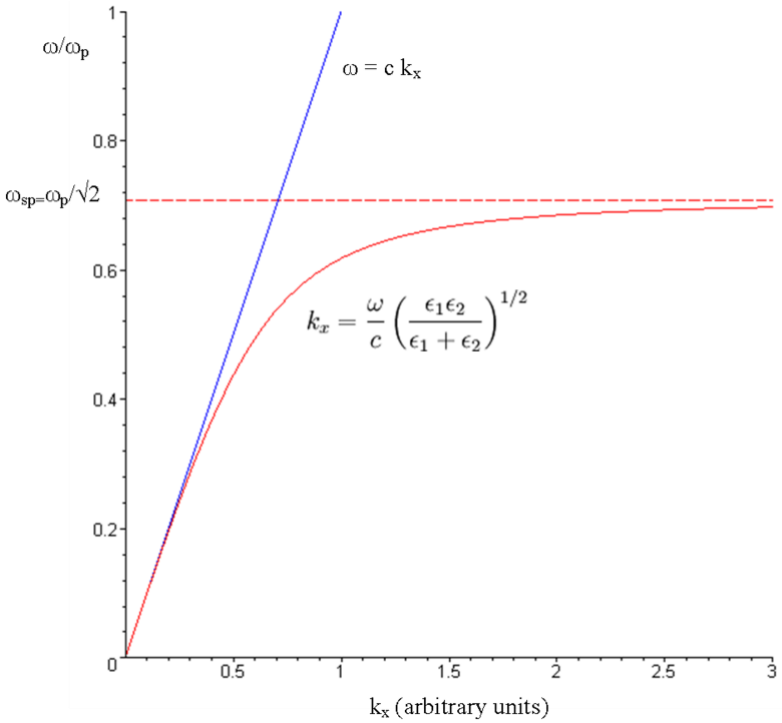

Fig 2. 4 : Dispersion curve of Plasmon[30]

From figure 2.4 we can observe that for low value of k, SPP is going behave similar to photons. As the k increases the dispersion increases and reaches asymptotic limit called surface Plasmon frequency ω_{sp}.

$\omega_{sp} = \omega_p / \sqrt[2]{1+} \varepsilon 2$

Due to the presence ohmic losses and electron core interactions damping is observed during the propagation of the wave.

Propagation length and skin depth

SPP loose its energy while propagating along the metal surface via absorption in to the metal surface. The decay is inversely proportional to the square of electric field.
The propagation length defined to be the distance for the SPP intensity decay to the factor of 1/e.

Condition is fulfilled at length L which is defined as

$$L = \frac{1}{2k''z}$$

Similarly, electric field is evanescently perpendicular to the metal interface.
The decay can be showed by skin depth formula for metal and dielectric.

2.4. Applications of Plasmonics

SPPs may be used for guiding the light efficiently in to nanoscale structures. One key advantage of plasmonic devices is that they have the ability to confine electromagnetic oscillations at optical frequencies to volumes that are much smaller than the wavelength that would be generated in free space at that frequency. This is useful for the generation of light by devices much smaller than the wavelength, as in plasmonic lasers such as spasers (surface Plasmon lasers). It is also useful for creating extremely intense, concentrated electromagnetic fields at optical frequencies, such as in optical antennas. Such high intensities are necessary for applications like single-molecule spectroscopy (e.g. SERS, Surface-Enhanced Raman Spectroscopy).
The extreme confinement of light beyond normal optical limits (such as the diffraction limit) can also be useful in areas like lithography and microscopy, for increased resolution and sensitivity.

Chapter 3

PERFECT ABSORPTION

3.1. Introduction

Nanostructure can absorb light for TM and TE polarization exited absorber and across entire visible spectrum. This structure can be used to convert absorbed light into usable energy. Absorber can be thought of as a device in which the radiation incident can be absorbed and all other processes such as reflection, transmission, scattering, and other light propagation are not possible. Salisbury screen which is a typical EM wave absorber developed by W. W. Salisbury is a basic example of the resonant absorber. This device consists of two layers,

1. Resistive heat to absorb EM wave
2. Metal plate to reflect the wave

Another example can be Dallenbach absorber in this a homogenous layer in front of mental plate. Crossed Grating absorber uses reflective one more type of absorber unit cell is three layered structure in which contains two metal layers, one bottom sheet and shape varying electric ring resonator (ERR) set apart by dielectric sheet. The dielectric top layer supports the ERR to be coupled strongly to incident wave electric field and not so much strongly to the magnetic field, which leads to electric field dependent response. While the incident magnetic field leads to the penetration in the space between the ERR and back metal ground plane due to which frequency dependent magnetic response. We can adjust the ERR and tune the $\varepsilon(\omega)$ and $\mu(\omega)$. Hence the impedance matching for the absorber and free space can be achieved and reflections can be decayed almost to zero. Also, imaginary part of permittivity is changed to get greater loss and reduce the transmission almost to zero. The resulting absorption A, is calculated

$A(\omega) = 1-R(\omega)-T(\omega)$,

Where $R(\omega)$ is the refection and $T(\omega)$ is the transmission, nearly equal to zero.

The similar type of structure has been used in this thesis in which metal layer is composed of the silver (Ag), both top and bottom layers are made up of silver while the dielectric/insulator layer is of silica (SiO_2).

3.2. PERFECT ABSORBERS: OPERATIONAL PRINCIPLE

Operational principles of thin perfect absorber can be understood in terms of effective electric and magnetic-current sheets which model the polarization and conduction currents induced in the respective composite structures. Figure 3.1 illustrates a generic composite layer illuminated by a normally incident plane wave. The layer thickness is assumed to be optically small, so that the layer can be considered as a metasurface: a microscopically structured sheet (usually periodic) with the period of the structure smaller than the wavelength in the surrounding media. This restriction on the period is necessary to ensure that the absorbing layer does not generate diffraction lobes, and for an observer in the far zone the response is that of an effectively homogeneous sheet. Another restriction on the geometry of the layer is that it can be asymmetric with respect to the two sides; it can be asymmetric with respect to mirror inversion (chiral) or have nonreciprocal elements (magnetized ferrite or plasma inclusions). Under the assumption of an electrically small thickness and the period smaller than the wavelength, the reflected and transmitted waves are plane waves created by the surface-averaged electric- and magnetic-current sheets Je and Jm, respectively, as illustrated in Fig.3.1.

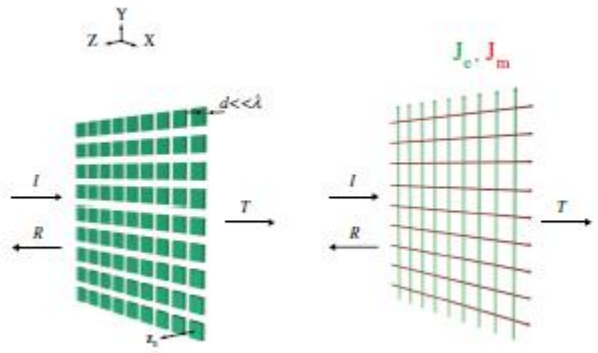

Fig 3. 1: Geometry of ultrathin absorbing layer[30]

(left) and its equivalent model for two current sheets (right).

In composite sheets, the layer has a complicated microstructure, usually containing some electrically small but resonant inclusions (like split rings). The surface-averaged current densities can be related to the electric and magnetic dipole moments p and m induced in each unit cell as

$$J_e = \frac{j\omega p}{S}$$

$$J_m = \frac{j\omega m}{S}$$

Here S is the unit-cell area and time-harmonic convention exp(jωp) is used. The higher-order multipoles induced in the unit cells do not contribute to the radiated plane-wave fields of the infinite array (higher-order modes are important in calculations of the dependence of the induced averaged currents on the incident fields). In this overview, we describe thin composite layers acting as perfect absorbers, that is, layers which have
zero-reflection and transmission coefficients: R = T =0.

3.3 Broadband Perfect Absorbers and Resonant Perfect absorbers

Perfect EM-wave absorbers can be divided into two groups;

(i) Broadband absorbers

(ii) Resonant absorbers.

Until now, the resonant absorbers were capable of perfect absorption in a narrow bandwidth, while only non-resonant techniques were used for broadband absorption. It is possible to make resonant absorbers operating in a broad range of frequencies by stacking multiple layers. However, these kind of broadband absorbers are very thick and bulky.

The resonant absorbers can have broadband behavior without above mentioned disadvantages as well.

Broadband Perfect Absorbers

The broadband absorbers are further divided into two categories: geometric transition absorbers and low-density absorbers.

In real application of Perfect absorber, it is desirable to be broadband, for TE and TM polarization of incident EM waves, and independent of the angle of incidence. If the Perfect Absorber is flexible it is even better.

Consider an EM wave impinging normally on a planar boundary of medium, in the most general case, with complex permittivity and permeability. The medium is surrounded by the free space or at least air. The (complex) reflection coefficient is

$$\Gamma = \frac{z-z0}{z+z0}$$

Where $z = \frac{\varepsilon}{\mu}$ is impedence of the medium and $z_0 = \frac{\varepsilon 0}{\mu 0} = 377\ \Omega$

For perfect reflection the absolute magnitude of impedance z is either 0 or infinity.

The impedance with zero magnitude can be achieved by using a metal plate. Frequency-selective surface (FSS) can be an example of medium with the impedance of 'effectively' infinite magnitude. To be Perfect Absorber the reflection should be 0. If $z = z_0$ then r = 0. This condition is called impedance matching, at which the travelling wave cannot 'see' the reflecting boundary. To make absorption better than 99% reflection coefficient |r| should be less than 0.1. One of the most important factors limiting the small enough reflection on a broad range of frequency is the dispersion of z.

Usually z is depending on frequency of incident EM wave. Hence, the strength of dependence on frequency is very important for the performance of broadband absorption. If the impedance is very weakly dependent upon the frequency in a wide range of frequency and is close to that of free space, the reflection would be very small in a wide range of frequency. If the angle of incidence is not zero, i.e., oblique incidence, the reflection coefficient is dependent not only on the angle of incidence but also on the polarization. Zero reflection can be achieved at least at one angle of incidence and at a particular orientation of the electric field of incident EM wave. The reflection is usually non-zero for the other direction of polarization. That is why it is not a simple job to make a polarization-independent omni-directional zero reflector. Another important factor is the material property of the absorbing medium. Even if a perfect impedance matching is achieved, the energy of the transmitted radiation should be dissipated efficiently in the interior of medium. Otherwise, the absorbed energy will be re-emitted in the form of radiation. Therefore, materials used in the broadband Perfect Absorber must have high electric and magnetic losses.

Geometric-Transition Absorbers

Geometric-transition absorber consists of two-dimensional periodic arrays of lossy-foam pyramids, cones or wedges, and is widely used in anechoic rooms to minimize the reflections from walls. Frequency-selective surface is a 2-dimensional periodic array of metallic patches, which have a particular shape for optimum operation. The screen on a microwave oven is an

example. FSS is, depending on the usage, designed to reflect, transmit, or absorb EM waves based on frequency. The operating frequency is determined by the size of the unit cell.

Resonant Perfect Absorbers

Resonant Absorbers uses the quarter wavelength width of substrate prior to ground metal plate. It has three layers:

(i) Thin resistive plane

(ii) Low-loss dielectric substrate with quarter wavelength width

(iii) Metal Surface

Now if considering EM wave passes by the resistive plane first and then gets reflected by the metal surface and after getting reflected reaches to resistive field, then the distance covered by EM wave is half the wavelength which corresponds to 180^0 phase shift. Due to this shift there is destructive interference.

Short circuit present at metal plate converted to open circuit as it reaches resistive screen by quarter-wavelength transmission line. If resistive screen has impedance as that of the free space, then no reflections occurs and hence maximum absorption is possible.

CHAPTER 4

METHODS

4.1. INTRODUCTION

Various techniques can be used to find the solution of the Maxwell's equation like Finite Difference Time Domain Method, Finite Element Method, Finite Element Method and Method of Moment etc. A commercial software uses any of these techniques to calculate the response.

Following methods can be used to study the reflection properties of the designed nanostructure:
Finite Element Method
Finite Difference Time Domain Method

4.2. Finite Element Method

FEM (Finite element Method) is technique to calculate the solution to boundary value problems (i.e. the problems in which certain conditions are forced on the boundaries) for partial differential equations. In FEM method, the desired spatial area for the problem is represented as smaller mesh or grid. The grid can be chosen to be of 2d triangular shape or any other form. Mesh can be chosen as 3d shape as well like tetrahedral, prism or pyramid.
Next step is to choose the basis function.

The basic algorithm for FEM is given as below –

1. To discretize into finite entities called finite element. Elements are connected to each other by the nodes, together they are known as mesh.
2. Derive simpler element equations. If value of a variable is known at nodes of an element, then value of the variable at any point within the element can be approximated by using the equation defined for element (equation can be polynomial and is called interpolation function). The actual equation might be more complex for the element; however approximate known equation is chosen.
3. Assemble/Combine the equations.
4. Apply Boundary conditions.

5. The equations are solved using the nodal values of dependent variables and shape functions throughout. Piece-wise approximated solution is calculated for the problem.
Numerical results presented in this report have been obtained in a commercial software COMSOL Multiphysics© which is based on Finite Element Method.

4.3. Finite Difference Time Domain Method

Though not used for the work presented in this report, we find it necessary to give a brief introduction of Finite Difference Time Domain Method. It involves discretization of Maxwell's equations in space and time using central difference formula.
Starting from Taylor's expansion

$$f(x_0 + \Delta x) = f(x0) + \frac{df}{dx}\Big|(x = x_0)\Delta x + \frac{d^2f}{dx^2}\Big| (x = x_0)\ (\Delta x)^2 + \frac{1}{3!}\frac{d^3f}{dx^3}|x = x_0(\nabla x)^3$$

Then the spatial domain is described where the simulation is supposed to be done. Spatial domain is divided in to elements. Differences are calculated on along element to get the complete solution.

From Taylor's Expansion, we can write the difference equation as follows-

$$f(x_i + \Delta x)|t_n + f(x_i - \Delta x)|t_n = 2f(x_i)\left|t_n + (\Delta x)^2 \frac{d^2f}{dx^2}\right|_{x_i t_n} + \frac{(\Delta x)^4}{12}\frac{d^4f}{dx^4}|x_i t_n$$

i and n are integers and mesh length is represented as Δx.
Second derivative can be calculated as follows –

$$\left|\frac{d^2f}{dx^2}\right|_{x_i t_n} = \frac{f(x_i+\Delta x)|t_n + f(x_i\Delta x)|t_n - 2f(x_i)|t_n}{(\Delta x)^2} + \Theta[(\Delta)^2]$$

And wave equation can be written as –

$$\frac{d^2u}{dx^2} = \frac{1}{c^2}\frac{d^2u}{dt^2}$$

u can be E or H where E is electric field and H is magnetic field.

And the equation can be represented as

$$\frac{u_{i+1}^{n}+u_{i-1}^{n}-2u_{i}^{n}}{(\Delta x)^2}+\ \Theta[(\Delta x)^2]=\frac{1}{c^2}\left[\frac{u_{i}^{n+1}+u_{i}^{n-1}-2u_{i}^{n}}{(\Delta t)^2}+\ \Theta[(\Delta t)^2]\right]$$

Final difference equation can be written equation as –

$$u_{i}^{n+1}\cong\frac{u_{i+1}^{n}+u_{i-1}^{n}-2u_{i}^{n}}{(\Delta x)^2}(c\Delta t)^2-\ u_{i}^{n-1}-2u_{i}^{n}$$

Maxwell equations are solved using FDTD through Yee cell (as shown in figure 4.1), Electric field should be meet the equation

$$\frac{dE}{dt}=\frac{1}{\varepsilon}[\nabla\times H-(J+\sigma E)]$$

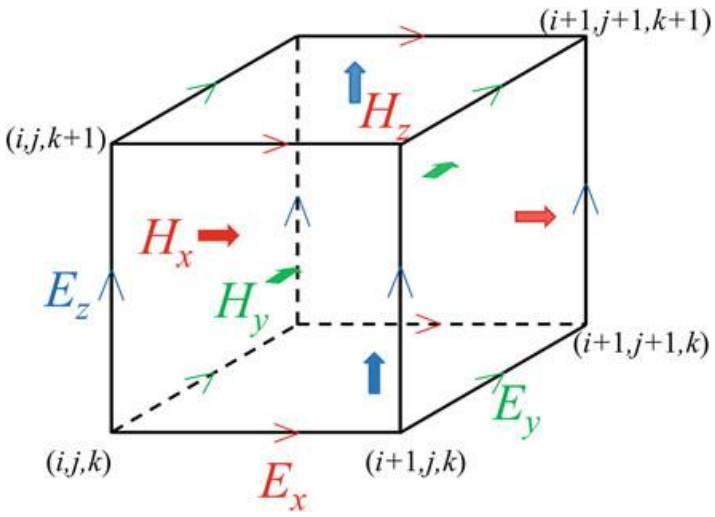

Fig 4. 1 : Cartesian cell for FDTD

Where σ is electrical conductivity and J is the current source. Different component of electric fields can be written as –

$$\frac{dE_x}{dt}=\frac{1}{\varepsilon}\left(\frac{dH_z}{dy}-\frac{dH_y}{dz}\right)-(J+\sigma E_x)$$

Now center difference can be written as

$$\frac{E^{n+\frac{1}{2}}_{x,\{i,j+1/2,k+1/2\}} - E^{n-\frac{1}{2}}_{x,\{i,j+1/2,k+1/2\}}}{\Delta t} = \frac{1}{\varepsilon_{x,\{i,j+1/2,k+1/2\}}}\left(\frac{H^{n}_{z,\{i,j+1,k+1/2\}} - H^{n}_{z,\{i,j,k+1/2\}}}{\Delta y} - \frac{H^{n}_{y,\{i,j+1,/2k\}} - H^{n}_{y,\{i,j+1/2,k\}}}{\Delta z}\right) - J^{n}_{x,\left\{i,j+\frac{1}{2},k+\frac{1}{2}\right\}} + \sigma_{\left\{i,j+\frac{1}{2},k+\frac{1}{2}\right\}} E^{n}_{x,\{i,j+1/2,k+1/2\}}$$

j and k represent integers here, y and z component of the electric field can be found likewise.

Using the below equation

$$\frac{df}{dt}|_{\cdot i\Delta x,\Delta y,k\Delta z,n\Delta t} = \frac{1}{\varepsilon}\left(\frac{f^{n+\frac{1}{2}}_{i,j,k} - f^{n-\frac{1}{2}}_{i,j,k}}{\Delta t}\right) + \Theta[(\Delta t)^2]$$

$$\frac{H^{n+\frac{1}{2}}_{x,\{i,j+1/2,k+1/2\}} - H^{n-\frac{1}{2}}_{x,\{i,j+1/2,k+1/2\}}}{\Delta t} = \frac{1}{\mu_{x,\{i,j+1/2,k+1/2\}}}\left(\frac{E^{n}_{z,\{i,j+1,k+1/2\}} - E^{n}_{z,\{i,j,k+1/2\}}}{\Delta y} - \frac{E^{n}_{y,\{i,j+1,/2k\}} - E^{n}_{y,\{i,j+1/2,k\}}}{\Delta z}\right) - M^{n}_{x,\left\{i,j+\frac{1}{2},k+\frac{1}{2}\right\}} + \sigma'_{\left\{i,j+\frac{1}{2},k+\frac{1}{2}\right\}} H^{n}_{x,\{i,j+1/2,k+1/2\}}$$

Where M the magnetization source if present and σ' represents magnetic conductivity.
The finer time step (Δt) and meshes (Δx, Δy and Δz) leads to solution very near to the accurate solution.

The steps cannot be chosen too fine as it will take lot of time and can be numerically unstable as well which is due to truncation during the processing. If steps are large, simulation will be fast but results won't be much accurate and not acceptable. So by Courant-Friedrichs-Lewy condition we choose steps to be of size

$$\Delta t = \frac{\Delta t}{\sqrt{Dc}}$$

D is spatial Dimension.

CHAPTER 5

Broadband light absorption using metallic nanowire based perfect absorbers

5.1. Introduction

The plasmonic nanostructures can absorb light but that is usually polarization dependent and do not cover the complete solar spectrum. In this project, the frequency 400-700 nm bandwidth is focused as this portion of the spectrum as most of the solar radiation is in the range, also the human visibility lies in this range. Also, the 1550 nm has been explored.

Solar cells are environment friendly but not efficient enough to replace fossil fuels. The cost of solar cell is high mostly because of high production cost of silicon semiconductor. Hence a thinner material around 300 nm would be better as compared to the present 1μm present material.

Although existing thinner solar cell cannot be much efficient as longer wavelength light is dispersed over a large distance, hence the thinner the structure of solar cell, lesser the light near the red side of the spectrum is absorbed. So to eliminate this, plasmonic nanostructures have been introduced which easily scatter light. Putting these structures on top of the solar cell, the rays falling on the cell can be turned 90^0 such they travel horizontally in the structure. Hence the complete width of the nanostructure can be utilized for the absorption process.

Nanostructures designed up till were unable to scatter light for broad range of frequencies and for only one polarization. In this project, Plasmonic structure has been implemented that can scatter and absorb the radiation in both TE and TM polarization for 400-700 nm solar spectrum. The absorption properties have been studies in infrared region as well. The 3D structure has rows of silver nanowires which are of length 300 nm. Width of the structure has been varied as 60 nm and 120 nm. Absorption occurs across the range of 400nm –700nm and peaks at 420 and 470 nm. The proposed design will absorb light for TE and TM polarization, polarization independent structure can be implemented as the trapezoidal rows are crossed with the another group of trapezoidal rows which are set at 90°. Although as the metal and dielectric structures converts the energy absorbed by photon to heat such implementation is not yet possible. On the contrary the semiconductors convert the energy absorbed by the photons to electricity. Yet

this technology is not implementable directly but we can use the same technique to semiconductors to increase their output.

5.2. Structure of Plasmonic Nanostructure

The designed absorber has three-layer metal – insulator –metal (MIM) structure in which the top metal layer is patterned. Two such thin-film MIM absorbers structures are illustrated as metal stripes shown in (Fig.5.1) and trapezoid grating shown in (Fig.5.2) that are periodically arranged by the x and y axis with a periodicity of 300 nm. The top and bottom silver (Ag) layers of the Metal-Insulator-Metal (MIM) stack are (60 nm,120 nm) and 100 nm thick, and the middle SiO_2 layer thickness is 60 nm. MIM absorber structures mentioned in this report ahead have the thicknesses of layers are the same as mentioned above.

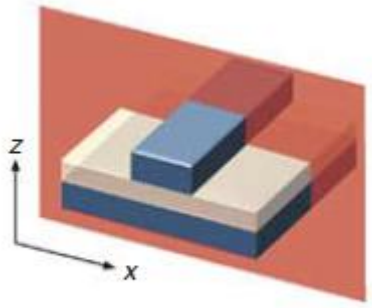

Fig 5. 1: 3D Rectangular metallic grating having cross-section area across x and y axis[29]

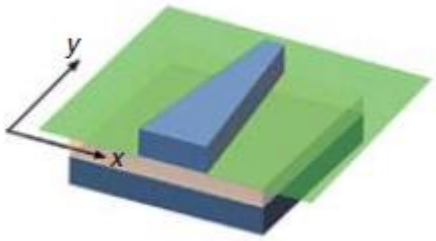

Fig 5. 2: 3D Trapezoid Metallic grating having cross-section area across x and y axis[29]

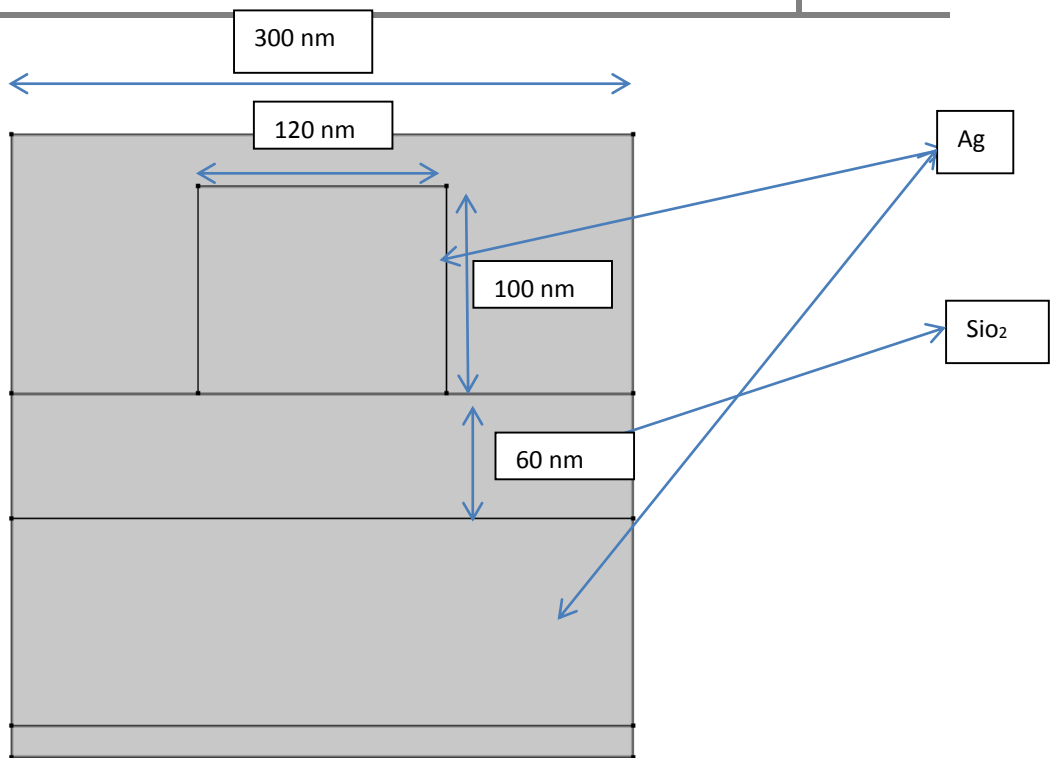

Fig 5. 3: 2D view of the structure designed in which upper layer as air and silver at top and bottom

The structure shown in Fig 5.3 has upper layer made up of silver and middle layer is composed of SiO_2 and bottom layer is of metal silver as well.

5.3. Method of Analysis

The proposed absorber structure is simulated using the commericially available software COMSOL multiphysics 4.3 which solves maxwell's equations using finite element method. This method of analysis has been discussed already in section 4.2.

5.4. Results and Discussion

The results have been simulated in 3D layout. The simulated results have been shown in the Fig 5.5,5.6 and 5.7.

Results for Metallic strips of w=60 nm and w=120 nm has been simulated. Extinction can be calculated as 1-T-R where T is transmission and R is reflection coefficient. The lower layer in the MIM stack hinders the transmission and making the extinction as 1-R as T is almost zero after putting up the thick silver layer at the bottom of the structure.

Figure 5.5 and 5.6 plots the simulated extinction spectra of the 60 nm (blue line) and 120-nm-wide (red line) metallic stripe arrays excited with TM polarization and TE polarization

respectively. Localized surface plasmon resonances can be distinguished from the extinction peaks in the spectra, and they yield narrow-band resonances depending on the width of the metal wire.

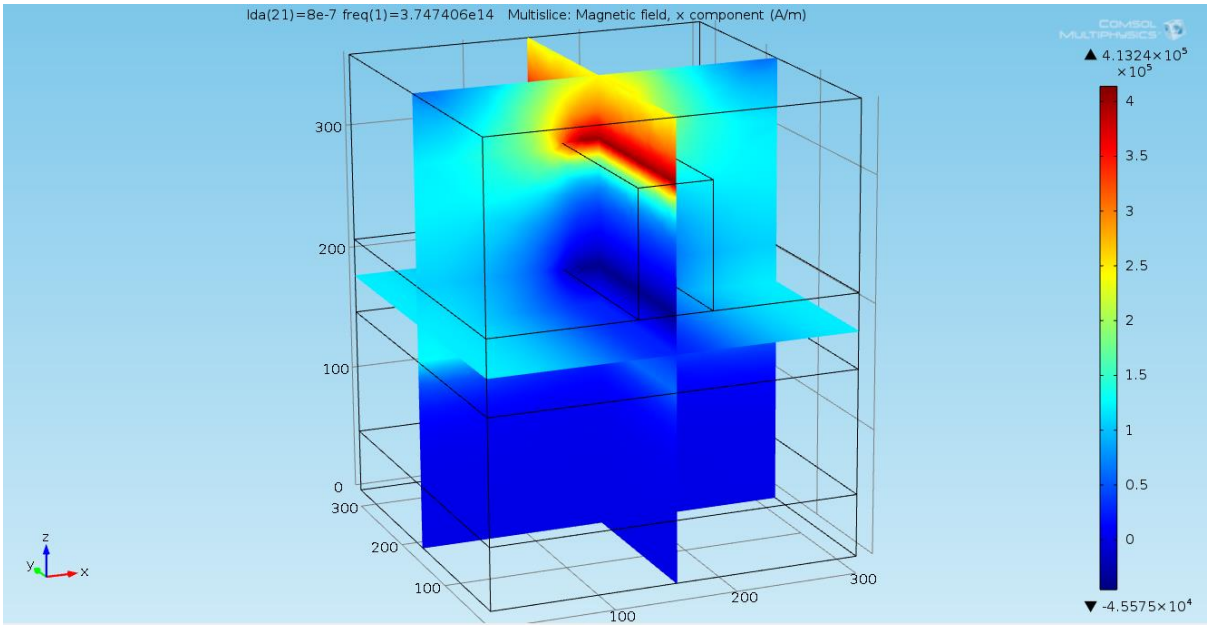

Fig 5. 4 :Electric field profile at the localized surface Plasmon resonance frequency.

The electric field profile shows that only negligible light is being received at other end. So, it can be concluded that designed structure is behaving as perfect absorber.

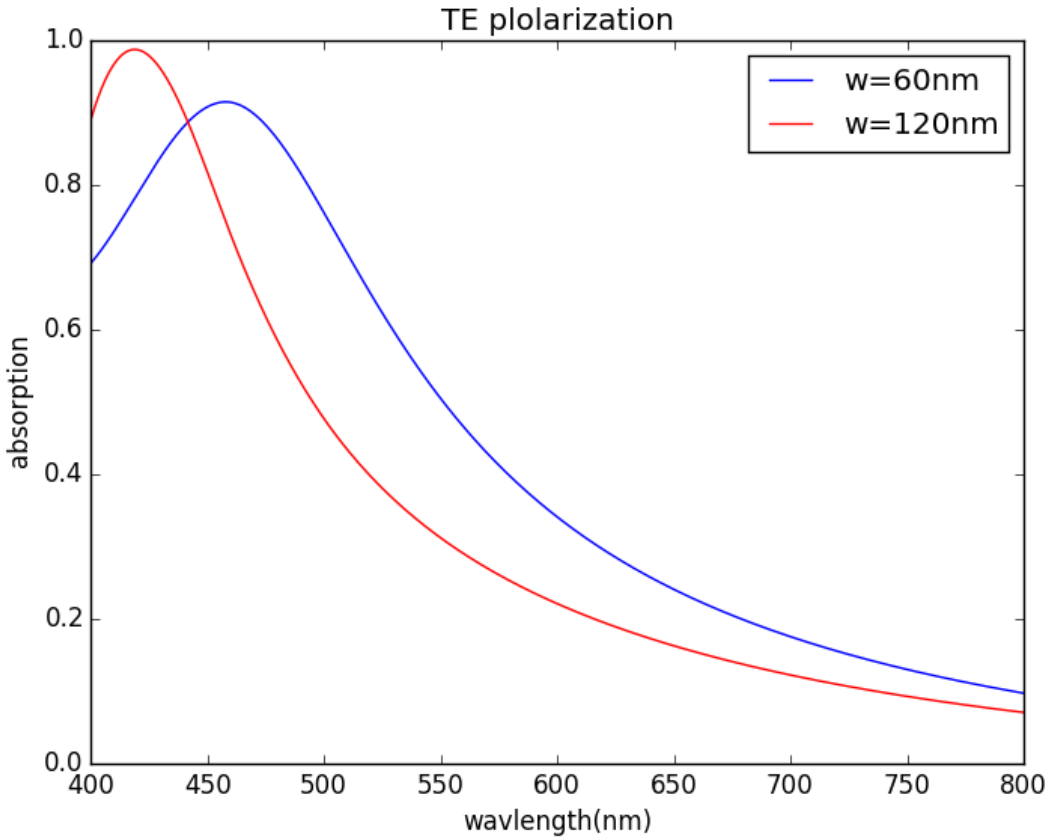

Fig 5. 5: Simulated absorption spectra for designed structure for TE polarization.

Above diagram shows absorption spectra for TE polarization, the structure length is 300nm and width is 60 nm (blue) and 120 nm (red).

Figure 5.5 plots the simulated absorption spectra of the 60 nm (blue line) and 120-nm-wide (red line) metallic stripe unit cell excited with TE polarization. Localized surface plasmon resonances can be observed from the extinction peaks in the spectra, and they typically yield narrow-band resonances depending on the width of the metal wire. As expected, the localized surface plasmon resonance redshifts with increased wire width.

For the 60 nm wide metallic stripe array, the resonance peak is observed at 420 nm with the maximum extinction value of 0.99 and for the 120 nm wide stripe the maximum extinction is 0.92 measured at 470 nm.

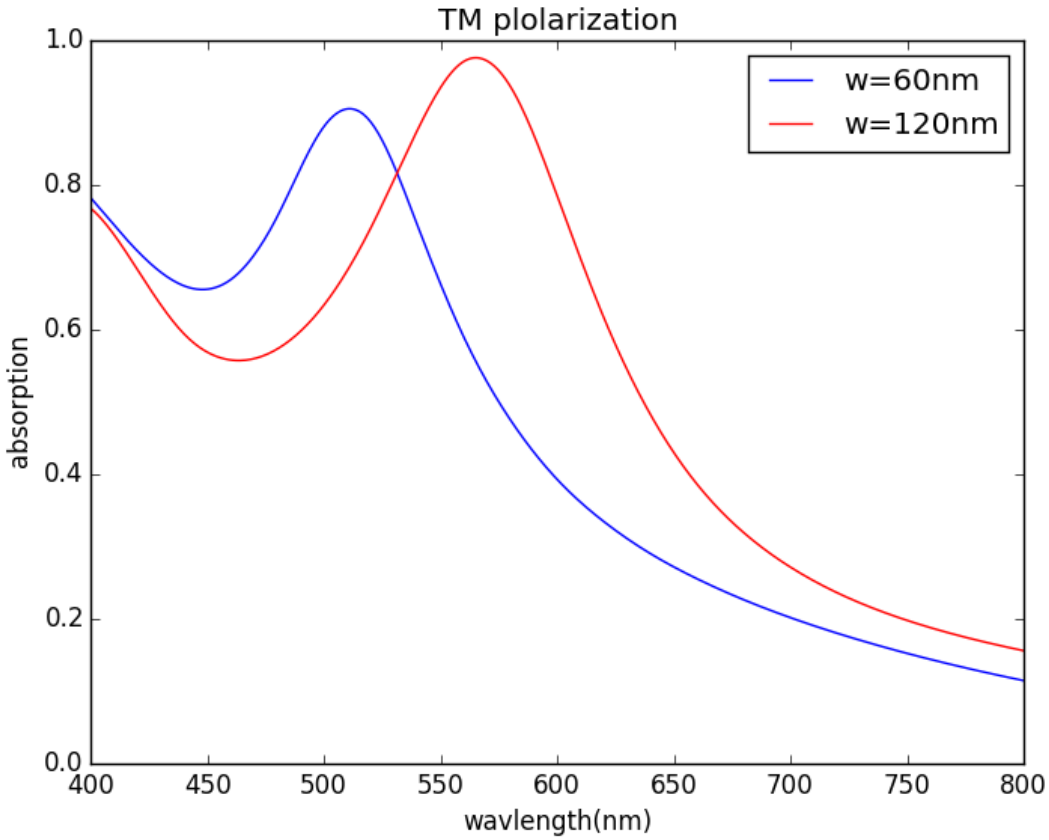

Fig 5. 6: Simulated absorption spectra for designed structure for TM Polarization.

Above figure shows absorption spectra for TM polarization, the structure length is 300nm and width is 60 nm (blue) and 120 nm (red). The absorption peaks at 420 nm (0.99) for w = 60 nm and at (0.92) at 470 nm.

Figure 5.6 plots the simulated absorption spectra of the 60 nm (blue line) and 120-nm-wide (red line) metallic stripe unit cell excited with TM polarization. Localized surface plasmon resonances can be observed from the extinction peaks in the spectra, and they typically yield narrow-band resonances depending on the width of the metal wire. As expected, the localized surface plasmon resonance redshifts with increased wire width.

For the 60-nm-wide metallic stripe array, the resonance peak is observed at 500 nm with the maximum extinction value of 0.92 and for the 120-nm-wide stripe the maximum extinction is 0.99 measured at 507 nm.

.

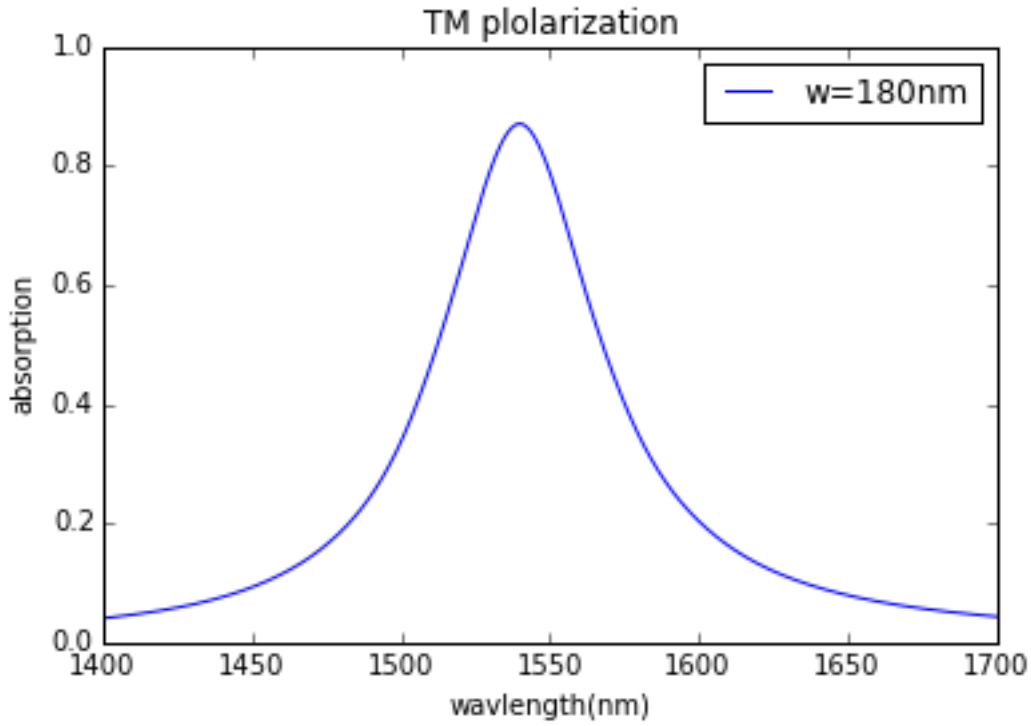

Fig 5. 7:: Simulated absorption spectra for designed structure for TM Polarization at w=180 nm.

Above figure shows absorption spectra for TM polarization, the structure length is 300nm and width is 180 nm. The absorption peaks at 1550 nm (0.90).

Figure 5.6 plots the simulated absorption spectra of the width w=180 nm. Localized surface plasmon resonances can be observed from the extinction peaks in the spectra, and they typically yield narrow-band resonances depending on the width of the metal wire. As expected, the localized surface plasmon resonance redshifts with increased wire width.

Chapter 6

Conclusion and Future Scope

6.1. Conclusion

In this project, we have designed and analysed a metallic nanowire based absorbers for resonant light absorption. To obtain the high absorption, We have used a 100nm thick silver (Ag) back reflector at the bottom layer that prevents the MIM structure from transmitting the light and decreases the factor 1-R. The structure shows the extinction of 0.10 with low transmission. We have proposed a structure with varying length to make the absorption polarization independent, as for the structure designed still have the dependency on the polarization. The variation of length i.e trapezoid structure can be used to give the polarization independent results for absorption.

The simulated results indicate that the MIM structures can be used to absorb the light in wide range. Thus we can conclude that ultrathin structures perfect absorbers can be designed which can further be utilized in several other fields like solar power harvesting.

6.2. Future Scope

Ultrathin plasmonic absorbers has high potential applications in Solar harvesting in future and can increase the efficiency of solar cells. It would be possible to absorb the wide range irrespective of the polarization.

References

1. Hutley, M.C. & Maystre, D. Total absorption of light by a diffraction grating Opt. Commun. 1 9, 431 – 436 (1976).
2. Bonod, N, Tayeb, G, Maystre, D., Enoch, S. & Popov, E.Total absorption of light by lamellar metallic gratings. Opt. Express 16, 15431 – 15438 (2008).
3. Christ, A. et al. Interaction between localized and delocalized surface plasmon polariton modes in a metallic photonic crystal, Phys. Status Solidi B 2 43, 2344 – 2348 (2006).
4. Christ, a.et al. Near-field-induced tunability of surface plasmon polaritons in composite metallic nanostructures. J. Microsc.2 29, 344 – 353 (2008).
5. Hibbins, A.P. et al. Resonant absorption of electromagnetic fields by surface plasmons buried in a multilayered plasmonic nanostructure. Phys. Rev. B 74, 073408 (2006).
6. Cesario, J., Quidant, R., Badenes, G. & Enoch, S. Electromagnetic coupling between a metal nanoparticle grating and a metallic surface. Opt. Lett. 30, 3404 – 3406 (2005).
7. Teperik, T. V. et al. Omnidirectional absorption in nanostructured metal surfaces. N at. Photonics 2, 299 – 301 (2008).
8. Le Perchec, J., Quemerais, P., Barbara, A. & Lopez-Rios, T. Why metallic surfaces with grooves a few nanometers deep and wide may strongly absorb visible light. Phys. Rev. Lett. 100, 066408 (2008).
9. White, J. S. et al. Extraordinary optical absorption through subwavelength slits. Opt. Lett. 34, 686 – 688 (2009).
10. Landy, N. I., Sajuyigbe, S., Mock, J. J., Smith, D. R. & Padilla, W. J. Perfect metamaterial absorber. Phys. Rev. Lett. 100, 207402 (2008).
11. Tao, H. e t al. A metamaterial absorber for the terahertz regime: design, fabrication and characterization. Opt. Express 1 6, 7181 – 7188 (2008).
12. Avitzour, Y., Urzhumov, Y. A. & Shvets, G. Wide-angle infrared absorber based on a negative-index plasmonic metamaterial. Phys. Rev. B 79, 045131 (2009).
13. Liu, X. L., Starr, T., Starr, A. F. & Padilla, W. J. Infrared spatial and frequency selective metamaterial with near-unity absorbance. Phys. Rev. Lett. 1 04, 207403 (2010).
14. Liu, N., Mesch, M., Weiss, T., Hentschel, M. & Giessen, H. Infrared perfect absorber and its application as plasmonic sensor. Nano Lett. 1 0, 2342 – 2348 (2010).
15. Greff et, J. J. et al. Coherent emission of light by thermal sources. N ature 4 16, 61 – 64 (2002).
16. Ferry, V. E., Sweatlock, L. A., Pacifi ci, D. & Atwater, H. A. Plasmonic nanostructure design for effi cient light coupling into solar cells. Nano Lett. 8, 4391 – 4397 (2008).
17. Atwater, H. A. & Polman, A. Plasmonics for improved photovoltaic devices. Nat. Mater. 9, 205 – 213 (2010).
18. Pala, R. A., White, J., Barnard, E., Liu, J. & Brongersma, M. L. Design of plasmonic thin-fi lm solar cells with broadband absorption enhancements. Adv. Mater. 2 1, 3504 – 3509 (2009).
19. Aubry, A. et al. Plasmonic light-harvesting devices over the whole visible spectrum. Nano Lett. 1 0, 2574 – 2579 (2010).
20. Narimanov, E. E. & Kildishev, A. V. Optical black hole: broadband omnidirectional light absorber. Appl. Phys. Lett. 9 5, 041106 (2009).
21. Wu, C. et al. Near-unity below-band-gap absorption by microstructured silicon. Appl. Phys. Lett. 78, 1850 – 1852 (2001).
22. Huang, Y. F. et al. Improved broadband and quasi-omnidirectional antireflection properties with biomimetic silicon nanostructures. Nat. Nanotechnol.2, 770 – 774 (2007).

23. Yang, Z. P., Ci, L. J., Bur, J. A., Lin, S. Y. & Ajayan, P. M. Experimental observation of an extremely dark material made by a low-density nanotube array. Nano Lett. 8, 446 – 451 (2008).
24. Mizuno, K. et al. A black body absorber from vertically aligned single-walled carbon nanotubes. P roc. Natl Acad. Sci. USA 1 06, 6044 – 6047 (2009).
25. Garcia-Vidal, F. J., Pitarke, J. M. & Pendry, J. B. Effective medium theory of the optical properties of aligned carbon nanotubes. Phys. Rev. Lett. 78, 4289 – 4292 (1997).
26. Dolling, G., Enkrich, C., Wegener, M., Soukoulis, C. M. & Linden, S. Simultaneous negative phase and group velocity of light in a metamaterial. Science 3 12, 892 – 894 (2006).
27. Rakic, A. D., Djurisic, A. B., Elazar, J. M. & Majewski, M. L. Optical properties of metallic films for vertical-cavity optoelectronics devices. Appl. Opt. 37, 5271 – 5283 (1998).
28. Palik, E. & Ghosh, G. Handbook of Optical Constants of Solids II (Academic Press, 1999).
29. Broadband polarization-independent resonant light absorption using ultrathin plasmonic super absorbers Koray Aydin, Vivian E. Ferry, Ryan M. Briggs & Harry A. Atwater. Nature Communications 2011.
30.Thin Perfect Absorbers for Electromagnetic Waves: Theory, Design, and Realizations, Y. Radi, C. R. Simovski, and S. A. Tretyakov Phys. Rev. Applied 3, 037001 – 2015